Journal of Modern Researches on Electronic Defense Systems

Receive: 16 May 2025 Accept: 15 June 2025

# Design Electronic Defense Sensor of Photonic Crystal with Deep Learning

Behnam Dorostkar[1], Zohreh. Dorrani[2]*
Corresponding Author: dorrani.z@pnu.ac.ir

1. Department of Information and Communication, Amin Police University, Tehran, Iran.
2. Department of Electrical Engineering, Payame Noor University, Tehran, Iran.

**Abstract –** *This study introduces an innovative approach to enhance surface plasmon resonance (SPR) sensors by integrating photonic crystal structures with deep learning-based optimization. Addressing the research gap in comprehensive frameworks that simultaneously optimize geometric and material parameters, the methodology consists of defining structural parameters, generating a training dataset via FDTD electromagnetic simulations, training a deep autoencoder model, and implementing a multi-stage optimization process combining random search, gradient-based SLSQP, and genetic algorithms to achieve globally optimal sensor designs. Experimental results demonstrate that the optimized photonic crystal SPR sensor achieves a high sensitivity of 99.22 nm/RIU and excellent linearity ($R^2 = 0.9998$). A low limit of detection (LOD) of 245.92 ng/mL, alongside binding kinetics analysis, further confirms the sensor's capability for real-time monitoring of molecular interactions. The main innovation lies in the synergistic use of deep learning and photonic crystal engineering, enabling simultaneous optimization of multiple design parameters and significant performance enhancement. This sensor combines nanophotonic engineering and artificial intelligence to allow the development of defense systems with rapid detection capabilities, high precision, and optimized energy consumption.*

**Keywords:** Deep Learning, Electronic Defense Sensor, Photonic Crystal, Surface Plasmon.

## 1. Introduction

The quest for highly sensitive and real-time sensors [1-3] has propelled SPR [4] technology to the forefront of analytical methods. SPR's capacity to monitor subtle refractive index changes near a metallic surface has unlocked new possibilities in drug discovery, environmental surveillance, clinical diagnostics, and food safety. While conventional SPR systems have proven valuable, their limitations in detecting low-concentration analytes or discerning delicate molecular interactions have motivated the exploration of advanced strategies to boost their performance.

Photonic crystals [5, 6] (PhCs), with their unique to manipulate light at the nanoscale, present a compelling route to enhance SPR sensing. The integration of PhCs [7] into SPR platforms allows for precise control of surface plasmon waves, leading to sensors [8, 9] with enhanced resolution and lower detection limits. However, the design of PhC-based SPR sensors presents a formidable challenge, requiring meticulous control over numerous structural parameters.

To navigate this design complexity, machine learning [10] methodologies, especially deep learning [11] architectures, have emerged as indispensable tools. These algorithms [12, 13] can decipher intricate correlations between structural parameters and device performance, facilitating efficient exploration of the design landscape and identification of optimal configurations. The convergence of PhCs and deep learning [14] holds the promise of overcoming existing limitations and tailoring PhC-based SPR sensors for advanced sensing applications.

The incorporation of photonic crystal-enhanced SPR sensors is quickly being sought after in the field of electronic defence. In situations where the sensor monitoring of chemical or biological agents needs to be done at an early stage, these sensors offer high precision and reliability, the likes of which have never been seen before [15]. These sensors with such exceptional monitoring capabilities ensure that real-time identification is done with maximum precision never experienced before. Such sensors enable the process of measuring minute changes in refractive index, which is critical for sensing contaminants or signature threats that are usually ignored by standard monitors. Such features can be utilized in events like cutting off functionalities in weapons or critical infrastructure protection, which need speedy identification and precise risk evaluation to save casualties and avert disasters.

Photonic crystal-based SPR sensors can also actively serve the purpose of stealth technologies and electromagnetic interference. Such sensors designed from photonic crystal carry a quality springs to track faint electromagnetic field shifts thus allowing the identification of unused surveillance cameras or signal jamming devices. Such sensors owing to adversary mapping out electronic threats boast of sharp focus and extreme versatility making them unexplained tactics in the hand of defence personnel during electronic warfare [16]. In addition, the development and use of photonic crystal SPR sensors with machine learning algorithms is transforming the electronics defense system. Complex deep learning algorithms are used to analyze sensor information and automatically identify the class of threat and anticipate future electronic warfare strategies. The combination of these technologies with new materials increases not only the reliability of threat detection but also enables the development of intelligent systems that can adapt to complex and changing enemy actions. Therefore, photonic crystal-based SPR sensors will form the foundation of the next generation of electronic defense systems, which will be unparalleled in the detection and neutralization of new threats.

The growing use of SPR sensors in electronic warfare systems is due to their high sensitivity and flexibility. These sensors utilize functionalization techniques to alter the lattice geometry of photonic crystals, enabling detection of minute traces of neurotoxins or pathogens in real time. This capability is essential for early warning systems in battleground scenarios. This acts like the detection and removal of proteins, but in this instance, it deals with the more dangerous sarin gas, anthrax spores, etc.

Defect engineering in THz-range photonic crystals could enable the detection of subtle changes in dielectric materials. This, in turn, could help locate camouflaged vehicles or concealed communication systems. These sensors would also help maintain fuel purity standards in military aircraft, monitoring for propylene glycol sabotage. This serves both material verification and tampering defense functions essential to electronic defense systems, addressing anti-tamper and tamper-automated monitoring needs [17].

These sensors could also employ plasmonic coatings targeting explosive precursors like TNT to unmanned aerial vehicles for landmine detection. The machine learning optimization approach suggested in the study facilitates rapid recalibration to face new challenges such as novel energetic materials or electronic jamming signatures [18]. Such adaptability is what modern electronic defense systems desperately need, as reconfigurable hardware is redesigned at a slower rate than the pace at which threats change.

This work introduces a novel approach that leverages a deep autoencoder architecture to design and optimize PhC-based SPR sensors. This fusion of PhC properties and the capabilities deep learning [19] capabilities seeks to transcend the limitations of conventional SPR sensors, paving the way for groundbreaking advancements in sensing technologies.

## 2. Related Work

SPR technology has emerged as a powerful tool for real-time, label-free detection in diverse fields such as biosensing, environmental monitoring, and drug discovery. However, the performance of SPR sensors is highly dependent on their design and constituent materials. Researchers have explored various methods to enhance the sensitivity and reduce the detection limits of these sensors, including the use of innovative materials, advanced configurations, and machine learning algorithms.

Numerous studies have focused on improving SPR sensor performance through machine learning. For instance, Tadson et al. enhanced the accuracy of SPR angular detection by employing deep learning [20-23] to precisely determine plasmonic angles; their convolutional neural network (CNN) demonstrated significant improvements in measurement accuracy compared to traditional methods [24]. Chen et al. achieved high identification accuracy in fiber-optic SPR sensors by leveraging machine learning based on grayscale and RGB image features [25]. Moon et al. utilized machine learning to design meta-plasmonic biosensors based on metamaterials with negative refractive indices, substantially improving DNA detection sensitivity [26]. Liang et al. applied machine learning to SPR sensors for SARS-CoV-2 particle detection, achieving high accuracy and low detection limits[27]. Mondal et al. employed machine learning to accurately detect and classify DNA binding events on SPR biosensors [28]. Malinik et al. combined SPR imaging with machine learning to analyze carbohydrate microarrays and detect multiple sclerosis biomarkers in whole serum, thereby improving binding specificity and reducing cross-reactivity [29].

Beyond machine learning, novel materials and advanced configurations have also been investigated to enhance SPR sensor performance. Qian and Wang proposed a U-shaped long-range SPR sensor, which exhibits a lower detection limit and improved sensitivity compared to conventional SPR sensors [30].

In this study, the integration of the advantages of these two approaches is pursued through the design of a photonic crystal-based plasmonic sensor and the optimization of its architecture via a deep autoencoder framework. The proposed methodology involves defining structural parameters and performance metrics, generating training data via finite-difference time-domain (FDTD) simulations, training the deep autoencoder model, and conducting multi-stage optimization. The sensor's performance is evaluated using four analytical plots. By harnessing machine learning [31] for the design optimization of photonic crystal-based SPR sensors, this research seeks to achieve high sensitivity and low detection limits, advancing the frontier of SPR sensing technologies. This research contributes to the advancement of SPR sensor technology by addressing the following research gaps:

Deep Learning for Sensor Design: Unlike previous studies that primarily utilize deep learning for analyzing sensor output data, this work employs deep learning to directly design and optimize the sensor structure itself.

Photonic Crystal and Deep Learning Synergy: This research uniquely combines a photonic crystal structure with deep learning algorithms to simultaneously achieve high sensitivity and linearity in SPR sensors.

Multi-Stage Optimization Approach: The proposed method introduces a novel multi-stage optimization approach to find global optimal designs, which includes random search, the SLSQP algorithm, and a genetic algorithm.

The main innovation of this study lies in the integration of deep learning techniques with the design of photonic crystal-based SPR sensors to significantly enhance their performance. Specifically, a deep autoencoder architecture was employed for the optimization of the sensor structure, resulting in highly sensitive and rapid detection of refractive index changes. For the first time, a multi-stage optimization process—combining random search, gradient-based methods, and genetic algorithms—was applied to ensure the selection of a globally optimal sensor design from a functional perspective.

This approach enables the detection of threats at extremely low concentrations (such as explosive precursors or chemical agents) in electronic defense environments and can serve as a novel tool for real-time monitoring and rapid threat detection in surveillance and electronic countermeasure systems. Furthermore, the ability to process and analyze complex data using deep learning opens the door to the development of intelligent, self-learning sensors for a wide range of applications in defense and security industries

## 3. PROPOSED METHOD

For the structural design, the cross-sectional geometry shown in Figure 1 was utilized.

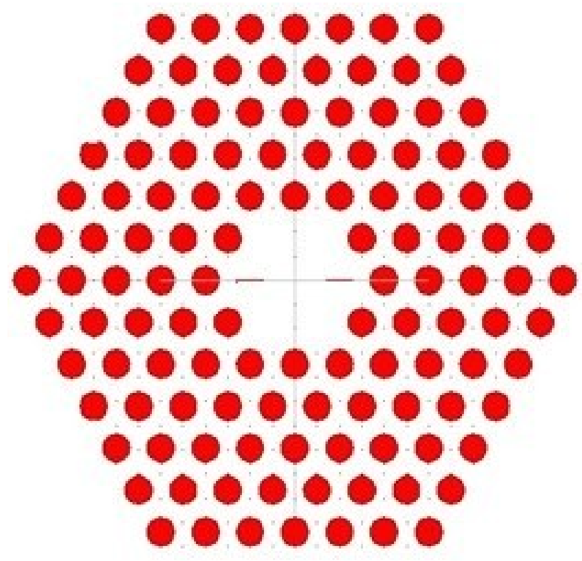

**Figure 1. cross-sectional sensor.**

The proposed photonic crystal has been defined a hexagonal structure composed of circular air holes arranged in a triangular lattice. This configuration was achieved by selective removal a subset of the central holes. The pseudo-code of the proposed method is provided below.

Pseudo-code of the Proposed Method

Start
Stage 1: Define parameters and performance criteria
    DEFINE structural parameters including:
        SET hole_radius to a range based on prior research
        SET rod_dimensions to a range based on prior research
        SET inter_hole_spacing to a range based on prior research
    SET material_properties to be learned using deep learning
    DEFINE performance metric as sensitivity.
Stage 2: Generate training data using FDTD simulations
    FOR each configuration in the structural parameters:
        SOLVE Maxwell's equations to calculate electric field (E) and magnetic field (B)
        COMPUTE resonant wavelength from the electric and magnetic fields
        COMPUTE loss spectrum from the electric and magnetic fields
        CALCULATE sensitivity using the resonant wavelength and the change in refractive index ($\Delta n$)
    END FOR
    CREATE a dataset with 1000 samples from the simulation results
Stage 3: Train deep autoencoder model

```
    NORMALIZE the dataset to prepare it for training
    BUILD an autoencoder model with the following structure:
        CREATE an input layer with size equal to the number of parameters
        ADD a dense layer with 64 units and ReLU activation function
        ADD a dropout layer with a rate of 0.2 to prevent overfitting
        ADD a dense layer with 32 units and ReLU activation function
        ADD a dropout layer with a rate of 0.2
        ADD an output layer with 1 unit to predict sensitivity
    CONFIGURE the model with the Adam optimizer and mean squared error loss function
    TRAIN the model on the normalized dataset for 100 epochs
     Stage 4: Perform multi-stage optimization
    STEP 1: Random Search
        GENERATE 500 candidate designs by randomly selecting parameter combinations
    STEP 2: Gradient-Based Optimization
        OPTIMIZE the candidate designs using SLSQP method, respecting physical constraints
    STEP 3: Genetic Algorithm
        USE the optimized candidate designs as the starting population
        SET mutation rate to 0.1 to introduce random changes
        SET crossover rate to 0.7 to combine designs
        USE the trained model's sensitivity prediction as the fitness score
        RUN the genetic algorithm to find the final optimized design
     Compute sensitivity of the optimized design
    SIMULATE the resonance shift (Δλ) for the optimized design
    DETERMINE the change in refractive index (Δn) from the optimized design
    CALCULATE the sensitivity using the formula S = Δλ / Δn
    RETURN the optimized design and its calculated sensitivity
End
```

To optimize the two-dimensional photonic crystal-based surface plasmon sensor, a deep autoencoder architecture was employed, and its implementation was conducted in four main stages.

Stage 1: Definition of Structural Parameters and Performance Criteria

Key geometric parameters—including the radius of the circular holes, the dimensions of the rods, and the inter-hole spacing—were defined based on prior research in two-dimensional photonic crystals. These parameters were organized in a hexagonal array with a triangular arrangement. The material composition of both the rods, and the background was determined via deep learning and was treated as material variables. The sensitivity (S) is defined by Equation 1:

$$S = \Delta\lambda / \Delta n \left[ nm / RIU \right] \quad (1)$$

Here, Δλ (in nanometers) is used to represent the resonant wavelength shift (e.g., absorption or reflection peak), and Δn denotes the refractive index change. The resonant wavelength in photonic crystals shifts with changes in the ambient refractive index (e.g., due to target molecule adsorption). Higher sensitivity enables the sensor to detect smaller refractive index variations.

Stage 2: Electromagnetic Simulation via FDTD.

FDTD simulations were used to solve Maxwell's equations for optical field calculations:

$$\begin{aligned} \nabla \times E &= -\partial B / \partial t \\ \nabla \times B &= \mu_0 J + \mu_0 \varepsilon_0 (\partial E / \partial t) \end{aligned} \quad (2)$$

Here, E represents the electric field, B denotes the magnetic field, $\mu_0$ the vacuum permeability, $\varepsilon_0$ the vacuum permittivity, and J correspond. The simulation outputs——namely, resonant wavelength and loss spectrum—served as the baseline data for training the deep learning model. The dataset included 1,000 samples of design parameters and their corresponding sensitivities, generated based on the nonlinear relationships between the parameters and the spectral response.

Stage 3: Deep Autoencoder Design

A deep neural network with an autoencoder architecture was designed, where normalized design parameters were used as inputs, and the predicted sensitivity were produced as outputs. The hidden layers employed the ReLU activation function:

$$h_1 = ReLU\left(W_1 X + b_1\right) \quad (3)$$

Here, X denotes the input vector, $W_1$ is the weight matrix of the first layer, and $b_1$ represents the bias vector. The ReLU function, defined as ReLU(z)=max (0, z), was applied element-wise. To prevent overfitting, dropout layers (rate = 0.2) were inserted between hidden layers. Training used the mean squared error loss function and the Adam optimizer.

Stage 4: Multi-Stage Optimization

The optimization began with random search in the design space, followed by the SLSQP algorithm to maximize the objective function. A genetic algorithm with mutation and crossover operators was integrated to avoid local optima. Sensitivity analysis quantified the impact of each parameter on sensor performance using Equation 1. Figure 2 illustrates the training and validation loss curves as a function of epoch during the training process.

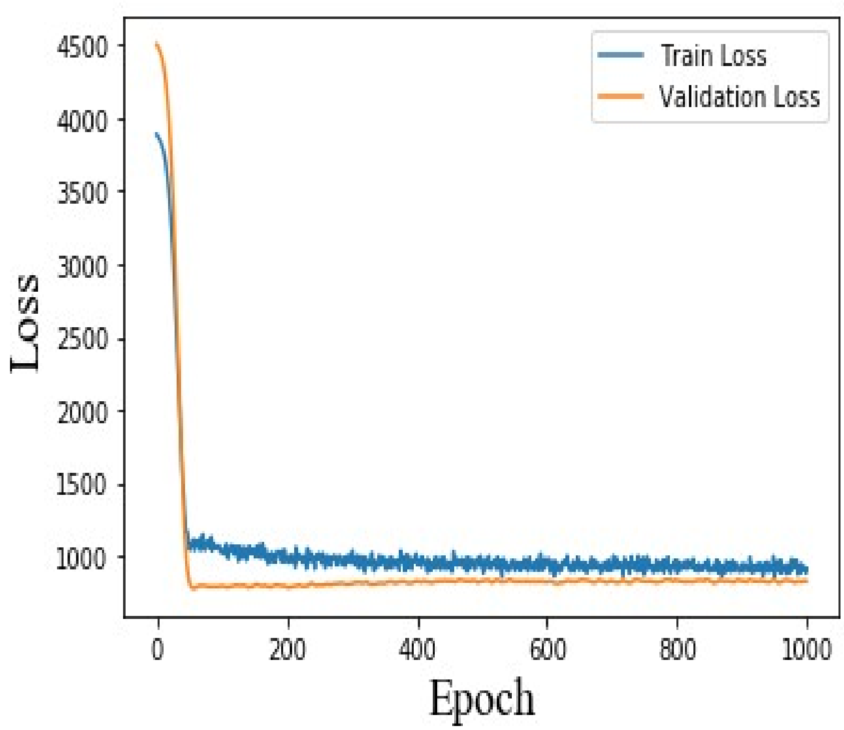


**Figure 2. Training and validation loss curves over 1000 epoch.**

At the beginning of training, both the training and validation losses start at a high value, decreasing rapidly within the first 1000 epochs. After this sharp decline, both losses stabilize and remain nearly constant for the remainder of the epochs, indicating that the model has converged and is no longer significantly improving or overfitting. The close alignment between the training and validation loss curves also suggests that the model generalizes well to unseen data.

**Table 1. Optimized parameters from the deep Autoencoder Algorithm**

| Parameter | Optimized Value (nm) |
|---|---|
| Hole Radius | 100.0 |
| Silver Rod Length | 50.0 |
| Silver Rod Width | 20.0 |
| Refractive Index | 2.00 |
| Inter-Hole Spacing | 200.0 |

Table 1 presents the optimized structural parameters for the photonic crystal-based SPR sensor. These values were obtained through the execution of a deep autoencoder algorithm, which efficiently explored the design space to identify the configuration that yields the maximizes sensitivity and linearity.

## 4. Result

The plots presented in Figure 2 provide a comprehensive analysis of the performance characteristics of the SPR sensor. As illustrated, key sensor parameters—including sensitivity, linearity, LOD, and response dynamics—are quantitatively assessed he calibration curve in Figure 3a shows the relationship between transmission loss, and wavelength for an optical system. The horizontal axis displays wavelength in nanometers (nm), and the vertical axis shows transmission loss. Each curve in this graph represents a different value of refractive index, which is indicated by the color bar on the side. As can be observed, with increasing refractive index, the curves shift toward higher wavelengths.

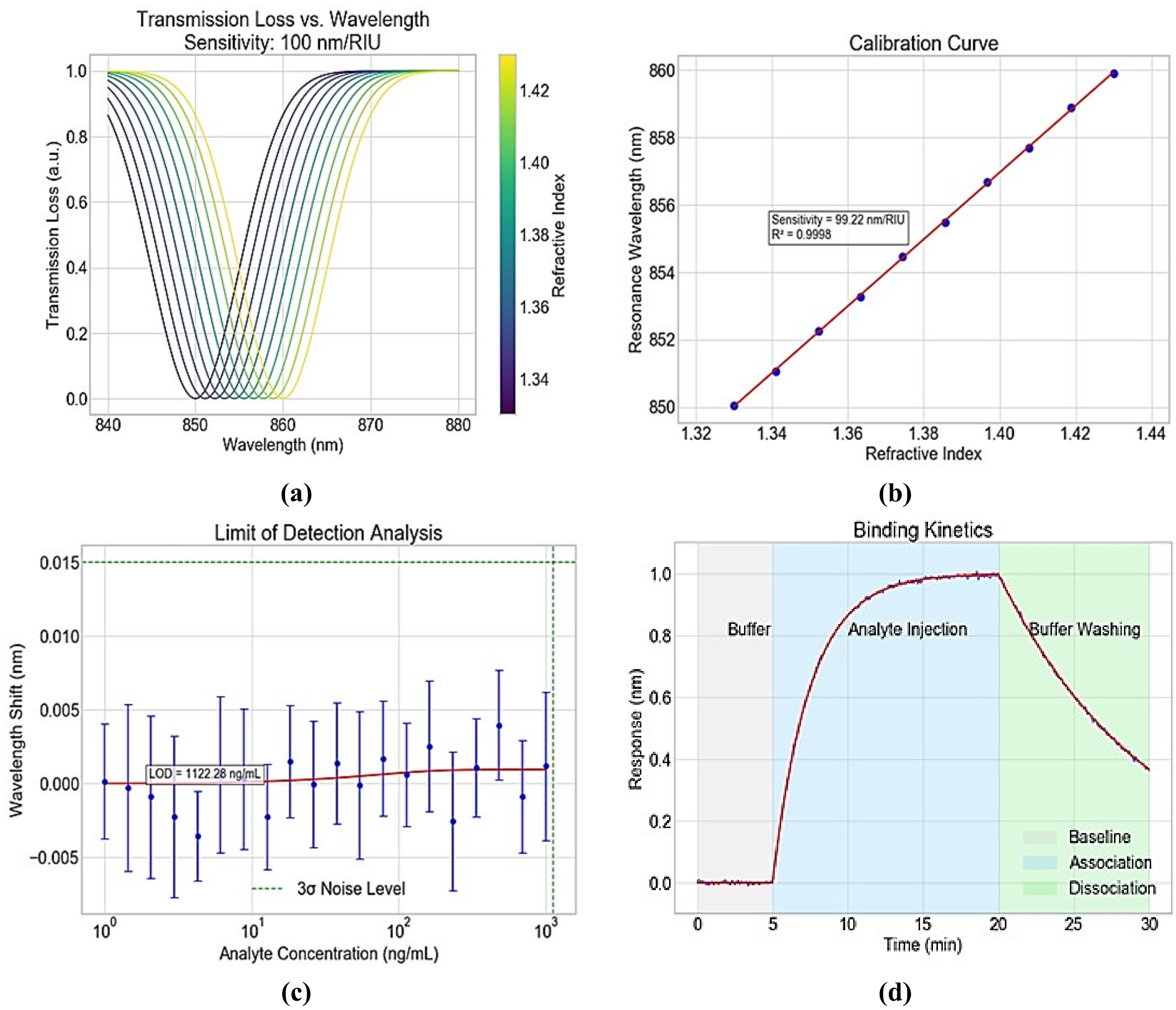


**Figure 3. Performance evaluation:(a) Transmission loss spectra versus wavelength for different refractive indices. (b) Calibration curve showing a linear relationship between refractive index and resonance wavelength, with a sensitivity of 99.22 nm/RIU and $R^2$ = 0.9998. (c) LOD analysis, indicating an LOD of 1122.28 ng/mL. (d) Binding kinetics plot illustrating baseline, association, and dissociation phases during analyte interaction.**

he calibration curve in Figure 3a shows the relationship between transmission loss, and wavelength for an optical system. The horizontal axis displays wavelength in nanometers (nm), and the vertical axis shows transmission loss. Each curve in this graph represents a different value of refractive index, which is indicated by the color bar on the side. As can be observed, with increasing refractive index, the curves shift toward higher wavelengths.

This graph examines the sensitivity of the system to changes in the refractive index of the surrounding medium. At the top of the graph, the sensitivity of the system is stated as 100 nanometers per refractive index unit (nm/RIU). This means that with a change in refractive index, the position of the minimum transmission loss (i.e., the resonance point) shifts significantly in wavelength, indicating the high sensitivity of the system to environmental changes. This feature is particularly important for applications such as material identification and biosensing.

The calibration curve in Figure 3b illustrates the linear relationship between the refractive index and the resonance wavelength. A calculated sensitivity of 99.22 nm/RIU, along with a coefficient of determination ($R^2$) of 0.9998, underscores the sensor's excellent linearity. Such linearity is crucial for accurate conversion of the sensor's signal into meaningful measurements, ensuring reliability in quantitative analysis. The LOD analysis in Figure 3c , calculated to be 245.92 ng/mL, demonstrates the sensor's capability to detect low concentrations of the analyte. A low LOD is particularly vital in applications such as biosensing, where the detection of minute amounts of target molecules is often required. Finally, the binding kinetics plot in Figure 3d depicts the various stages of the experiment: the baseline phase, the association phase, where the signal increases due to analyte molecules binding to the sensor surface, and the dissociation phase, where the signal gradually decreases as molecules detach. This plot not only validates the sensor's real-time monitoring capability, but also informs the optimization of experimental parameters, such as association and dissociation rates, leading to enhanced sensor performance The proposed method based on photonic crystals and deep learning, while maintaining high sensitivity (99.22 nm/RIU) and excellent linearity ($R^2$=0.9998), provides an adequate limit of detection (LOD ≈ 246 ng/mL) which is in the range of the articles mentioned. Also, The ability to analyze binding kinetics offers important benefits for the precise recognition and biosensing uses.

**Table 2. Compare proposed method**

| Refs | ML Algorithm | Performance/Results | SPR Sensor Setup | Machine Learning Application |
|---|---|---|---|---|
| **[24]** | Convolutional Neural Network | A convolutional neural network reached a measurement precision 4.23 × 10−6 RIU (66% more than traditional polynomial fitting) Sensitivity was ≈53.9° RIU−1 | SPR system using a nitrogen gas chamber to control refractive index changes | From deep learning, the measurement precision increase in the SPR angular detection for angular scanning by determining the plasmonic angle. |
| **[25]** | BP-NN, SVM | A detection limit of 0.9 nm for IgG, model recognition accuracy reaches 99.94 %. SPR RI resolution 6.3 × 10−5 RIU | SPR fiber-optic sensor, VIS and NIR CMOS sensors for image capture. | Application of ML for fibre optical SPR sensor RI detection |
| **[26]** | MLP, AE, t-SNE, and k-means clustering. | Over 13 times, increasing sensitivity compared to traditional SPR sensors. | SPR based on metamaterials. | Applying machine learning for metamaterial SPR biosensors with higher DNA resolution |
| **[27]** | Logistic regression, SVM | A LOD of 100 vp mL−1 and detection bandwidth ranges between 125.28–106 vp mL−1. The accuracy is above 97% | LSPR sensors for Au–TiO2–Au nanocups arrays with microscope imaging | Use of ML to detect and forecast coronavirus concetrations by using LSPR sensor images. |
| **[28]** | Random Forest (RF), SVM, DT, kNN, LR, and MLP | Random Forest and kNN aproaches reached best accuracy and up 0.96 for DNA detection | gold surfaces for DNA measurements 632.8 nm wave lenghth light. | ML to classify and ID DNA with SPR biosensors. |
| **[29]** | kNN, nnet | The range goes from 1 to 100 ng mL−1 LOD: 4.5–6.6 ng mL−1 Neural Network (94%) | Microarrays of cabohydrates covered by perfluorodecyltrichlorosilane (PFDTS) for detection of anti-ganglioside antibodies. | Combining SPRi analysis on microwires made of carbohydrates for the multiple sclerosis biomarkers |
| **[30]** | - | Lower Limit of Detection in comparison to ordinary SPR sensors, Sensitivity improved.(The precise numerical values are in the manuscript) | LRSPR sensor with U-shaped structure to increase resonance range | U-shaped Long-Range Surface Plasmon Resonance (LRSPR) Biosensor with Low Detection Limit |
| **Proposed Method** | Deep Autoencoder, SLSQP Algorithm, Genetic Algorithm | Sensitivity: **99.22** nm/RIU- Linearity: Coefficient of determination ($R^2$) is **0.9998**- LOD: **245.92** ng/mL | 2D Photonic crystal with a hexagonal structure composed of circular air holes arranged in a triangular lattice. The configuration was achieved by selectively removing a subset of the central holes. | Optimization of a Photonic Crystal-Based Surface Plasmon Sensor Using a Deep Autoencoder Architecture |

The LRSPR U-shaped sensor also significantly improves the LOD, which demonstrates the advancements achieved by the new sensor design. Overall, the integration of machine learning and structure optimization through the proposed method has enhanced sensor performance compared to existing approaches.

## 5. Electronic defense sensor applications

An electronic defense sensor, based on SPR integrated with photonic crystal structures and optimized through deep learning techniques, exhibits exceptional sensitivity and precision, making it highly suitable for advanced applications in modern electronic defense systems. Such systems demand rapid and accurate detection and monitoring of signals and environmental changes, which SPR–photonic crystal sensors effectively fulfill through their high sensitivity (99.22 nm/RIU) and excellent linearity ($R^2$ = 0.9998). The low LOD of approximately 245.92 ng/mL, along with their real-time monitoring capability of molecular interactions, enables swift and accurate detection of electromagnetic signals and environmental variations.

In electronic defense applications, these sensors can be employed for radar signal identification and analysis, detection of chemical or biological agents in military environments, and monitoring of electromagnetic field conditions. The multi-stage optimization approach—combining random search, gradient-based algorithms, and genetic algorithms—ensures that the sensor design achieves maximum efficiency and accuracy under diverse operational conditions. This synergistic integration of nanophotonic engineering and artificial intelligence–driven optimization allows for the simultaneous tuning of geometric and material parameters, significantly enhancing performance and reliability in complex and dynamic defense scenarios.

The integration of photonic crystal–based SPR sensors with unmanned aerial vehicles (UAVs) provides a strategic solution for rapid and remote detection of airborne chemical or biological threats in high-risk or inaccessible areas. Due to their compact size, lightweight design, and low power consumption, these sensors are highly suitable for onboard deployment on UAV platforms.

In chemical, biological, radiological, and nuclear threat scenarios, UAVs equipped with SPR sensors can perform autonomous monitoring without endangering human personnel. The sensor data is transmitted wirelessly to a ground station, where it is analyzed using AI-driven signal processing algorithms for real-time threat identification.

## 6. Conclusion

This study successfully demonstrated the design and optimization of a photonic crystal-based SPR sensor using a deep autoencoder architecture. The uniqueness offered by the optical characteristics of photonic crystals integrated with deep learning yielded high sensitivity of 99.22 nm/RIU, excellent linearity ($R^2$ = 0.9998), and noteworthy sensitivity (LOD = 245.92 ng/mL). These performance metrics highlight the sensor as a potential game changer for electronic defense systems where infrequent yet swift changes in electromagnetic fields, explosive precursors such as TNT, or fuel contamination demand immediate attention. The multi-stage optimization process employing random search, gradient-based approaches, and genetic algorithms was successful in designing stealth material detection and encrypted signal interference sensor designs.

The results underscore the potential of machine learning techniques to accelerate the development of SPR sensors for electronic warfare, including real-time monitoring of battlefield environments and counter-drone systems. The sensor's ability to resolve subtle refractive index shifts enables applications such as identifying dielectric variations in camouflaged vehicles or detecting low-concentration chemical agents in sabotage scenarios. Future work will prioritize experimental validation of the sensor in field-deployable electronic defense platforms, such as UAV-mounted surveillance systems or portable threat-detection kits. Additionally, we aim to explore federated learning architectures to enhance collaborative threat analysis across distributed defense networks and investigate terahertz-range photonic crystals for advanced electromagnetic cloaking applications.

## References

[1] M. Rahimnejad, R. A. Abd Alsaheb, and M. A. Atyia, "Current Developments in Biosensors for Monitoring Environmental Quality: A Critical Review," *International Journal of Engineering,* vol. 38, no. 4, pp. 921-936, 2025.

[2] Z. Dorrani and M. A. Mansouri-Birjandi, "Superlens Biosensor with Photonic Crystals in Negative Refraction," *International Journal of Computer Science Issues (IJCSI),* vol. 9, no. 3, p. 57, 2012.

[3] Z. Dorrani, "Biosensor for detection of biological components using photonic crystal," *Majlesi Journal of Telecommunication Devices,* vol. 12, no. 3, pp. 135-139, 2023.

[4] Z. Dorrani, "Designing Sensor based Surface Plasmon Resonance with Photonic Crystals," *Quarterly Journal of Optoelectronic,* vol. 1, no. 4, pp. 47-52, 2017.

[5] Z. Dorrani, "Negative Refraction, Subwavelength Lensing Effect and Total Mirror with a Photonic Crystal Structure," *Majlesi Journal of Electrical Engineering,* vol. 12, no. 1, pp. 55-60, 2018.

[6] Z. Dorrani, "Optical Supertrap with complete photonic lens," *Majlesi Journal of Telecommunication Devices,* vol. 4, no. 3, 2015.

[7] Z. Dorrani, "Simulation of Micro-Displacement Sensor Using Photonic Crystals," *Biquarterly Journal of Optoelectronic,* vol. 1, no. 2, pp. 17-22, 2016.

[8] Z. Dorrani, "Two-dimensional Photonic Crystal Sensor for Detection of Biomaterial," *Majlesi Journal of Electrical Engineering,* vol. 14, no. 1, pp. 25-28, 2020.

[9] A. Motamed, "Simulating the estimation of information of wireless sensors for use in all kinds of command and control networks," *New Researches in Electronic Defense Systems,* vol. 2, no. 3, pp. 41-48, 2023.

[10] O. Elharrouss, Y. Hmamouche, A. K. Idrissi, B. El Khamlichi, and A. El Fallah-Seghrouchni, "Refined edge detection with cascaded and high-resolution convolutional network," *Pattern Recognition,* vol. 138, p. 109361, 2023.

[11] M. Khodadadi, L. Riazi, and S. Yazdani, "A Novel Ensemble Deep Learning Model for Building Energy Consumption Forecast," *International Journal of Engineering,* vol. 37, no. 6, pp. 1067-1075, 2024.

[12] Z. Dorrani, "Road Detection with Deep Learning in Satellite Images," *Majlesi Journal of Telecommunication Devices,* vol. 12, no. 1, pp. 43-47, 2023.

[13] Z. Dorrani, H. Farsi, and S. Mohamadzadeh, "Deep Learning in Vehicle Detection Using ResUNet-a Architecture," *Jordan Journal of Electrical Engineering. All rights reserved-Volume,* vol. 8, no. 2, p. 166, 2022.

[14] Z. Dorrani, "Optimization of Photonic Nanocrystals for Invisibility Using Artificial Intelligence," *Journal of Advanced Materials in Engineering (Esteghlal),* vol. 44, no. 1, pp. 55-70, 2024.

[15] Y. Wang, Z. Wang, Y. Gao, J. Yan, Y. Chen, and L. Yang, "Three-dimensional photonic crystal optical gas sensor for trace detection and ultrafast response of chemical warfare agent in atmospheric humidity," *Talanta,* vol. 277, p. 126383, 2024.

[16] J. Wei, J. Yang, M. Qin, L. Yang, and S. Cao, "Designing a one-dimensional photonic crystal sensor for dimethyl methylphosphonate detection leveraging a hydrogen-bonding-based acidic strategy," *Sensors and Actuators B: Chemical,* vol. 423, p. 136722, 2025.

[17] Z. A. Zaky, M. Al-Dossari, V. Zhaketov, and A. H. Aly, "Defected photonic crystal as propylene glycol THz sensor using parity-time symmetry," *Scientific Reports,* vol. 14, no. 1, p. 23209, 2024.

[18] V. Fallahi, M. Hosseini, and Z. Kordrostami, "Optimization of highly sensitive three-layer photonic crystal fiber sensor based on plasmonic," *Physica Scripta,* vol. 99, no. 10, p. 105577, 2024.

[19] Z. Dorrani, H. Farsi, and S. Mohamadzadeh, "Shadow Removal in Vehicle Detection Using ResUNet-a," *Iranica Journal of Energy & Environment,* vol. 14, no. 1, pp. 87-95, 2023.

[20] Z. Dorrani, "Traffic Scene Analysis and Classification using Deep Learning," *International Journal of Engineering,* vol. 37, no. 3, pp. 496-502, 2024.

[21] M. Rohani, H. Farsi, and S. Mohamadzadeh, "Deep Multi-task Convolutional Neural Networks for Efficient Classification of Face Attributes," *International Journal of Engineering,* vol. 36, no. 11, pp. 2102-2111, 2023.

[22] M. E. ebrahim toosi and s. a. a. Izadi onji, "Estimation of channel profile and signal-to-noise ratio in wireless receivers using deep learning," *New Researches in Electronic Defense Systems,* vol. 3, no. 8, pp. 24-32, 2024.

[23] S. M. hasani azhdari and M. Khishe, "Pulse Repetition Interval Modulation Recognition and Classification Based on Deep Convolutional Neural Networks Improved with Extreme Learning Machine," *New Researches in Electronic Defense Systems,* vol. 2, no. 3, pp. 1-13, 2023.

[24] K. Thadson, S. Sasivimolkul, P. Suvarnaphaet, S. Visitsattapongse, and S. Pechprasarn, "Measurement precision enhancement of surface plasmon resonance based angular scanning detection using deep learning," *Scientific Reports,* vol. 12, no. 1, p. 2052, 2022.

[25] S. Chen, H. Wu, Y. Song, W. Peng, and Y. Liu, "A fiber-optic surface plasmon resonance sensor for bio-detection in visible to near-infrared images," *Biosensors,* vol. 12, no. 1, p. 9, 2021.

[26] G. Moon, J.-r. Choi, C. Lee, Y. Oh, K. H. Kim, and D. Kim, "Machine learning-based design of meta-plasmonic biosensors with negative index metamaterials," *Biosensors and Bioelectronics,* vol. 164, p. 112335, 2020.

[27] J. Liang, W. Zhang, Y. Qin, Y. Li, G. L. Liu, and W. Hu, "Applying machine learning with localized surface plasmon resonance sensors to detect SARS-CoV-2 particles," *Biosensors,* vol. 12, no. 3, p. 173, 2022.

[28] H. S. Mondal, K. A. Ahmed, N. Birbilis, and M. Z. Hossain, "Machine learning for detecting DNA attachment on SPR biosensor," *Scientific Reports,* vol. 13, no. 1, p. 3742, 2023.

[29] A. S. Malinick, D. D. Stuart, A. S. Lambert, and Q. Cheng, "Surface plasmon resonance imaging (SPRi) in combination with machine learning for microarray analysis of multiple sclerosis biomarkers in whole serum," *Biosensors and Bioelectronics: X,* vol. 10, p. 100127, 2022.

[30] Y. Qian and Q. Wang, "A U-shaped Long-Range Surface Plasmon Resonance (LRSPR) Biosensor with Low Detection Limit," *IEEE Sensors Journal,* 2024.

[31] H. SabbaghGol, H. Saadatfar, and M. Khazaiepoor, "Predicting Alzheimer's disease: A machine learning approach using advanced feature selection techniques," *Journal of Modern Medical Information Sciences,* vol. 10, no. 3, pp. 307-324, 2024.